Coherent Propagation of Femtosecond Optical Pulses in a Monoclinic ZnP_2 Single Crystal

Tomobumi Mishina and Yasuaki Masumoto
Institute of Physics, University of Tsukuba, Tsukuba, Ibaraki 305, Japan
(Received 2 July 1993)

The free induction decay signal from excitons in a ZnP_2 single crystal shows an unexpected temporal evolution, polariton beat, and coherent dip. We show that the effects come from a nonzero thickness of the sample and nonzero time width of the excitation pulses. A systematic numerical calculation provides good qualitative agreement with the data. These effects are very important in understanding the experimental results which deal with the coherent interaction between excitons and optical fields.

PACS numbers: 71.35.+z, 42.50.Md

Coherent transient spectroscopy has been widely used in investigations dealing with the interaction between light and matter. Recent developments in ultrafast laser techniques have enabled the observation of coherent effects of the exciton systems in semiconductors. Four wave mixing is a very important technique for observing the phase coherence time [1–4] and quantum beat effects caused by various mechanisms [5–8]. On the other hand, observation of the free induction decay (FID) signal is another important technique for studying coherent interactions. The FID signal was first observed by Hahn [9] for pulsed nuclear magnetic resonance and by Brewer and Shoemaker [10] for optical experiments. As a result of the short wavelength and directionality of the optical field, FID signals in optical experiments are sometimes referred to as coherent light propagation. Gibbs observed coherent propagation in atomic Rb and studied the nonclassical nature of a two-level system [11,12]. Fröhlich *et al.* pointed out the importance of the polariton propagation effect in Cu_2O [13] and a similar result in CdSe was reported by Pantke *et al.* [14].

In this work, we report on the femtosecond coherent pulse propagation in monoclinic ZnP_2 single crystals around the resonance region of $n=1$, 2, 3, and 4 excitons. ZnP_2 is one of the II-V compound semiconductors and its monoclinic form has a biaxial crystal structure. A monoclinic ZnP_2 crystal shows strongly anisotropic optical properties. For $E \parallel b$ polarization, a very sharp Wannier exciton series up to $n=7$ has been observed [15]. The fundamental properties of the excitons, such as the magneto-optical effects [16] and secondary emission [17], have been thoroughly studied. Thus the exciton system in a monoclinic ZnP_2 crystal is very suitable for studying the coherent interaction between light and the exciton system. We have observed the free induction decay signal and have found an exciton quantum beat, a polariton beat, and a coherent dip. Our experimental results show not only the importance of nonzero sample thickness but also that of the nonzero time width of optical pulses. We have also derived the simple equations for these phenomena in a systematic manner.

Single crystals of monoclinic ZnP_2 were grown from the vapor phase, and the as grown surfaces contain the b and c axes. The thickness of the sample used in this study is about 243 μm. Figure 1 shows the absorption spectrum of ZnP_2 crystals at 2 K for $b \parallel E$ polarization. Sharp exciton peaks up to $n=4$ are clearly observed.

In our experiments, we measure the time-resolved intensities of the femtosecond laser pulses transmitted through the sample. A femtosecond laser beam from a mode-locked titanium sapphire laser was separated by a beam splitter. The laser generates stable, tunable, and nearly Fourier-transform-limited pulses with a width of about 130 fs. One beam is transmitted through the sample in a cryostat and the other beam is time delayed by a corner cube reflector, and they are then mixed in an external nonlinear crystal. The optical mixing signal is measured as a function of the time delay.

Figure 2 shows the FID signal from the $n=2$, 3, and 4 excitons. A large peak at $t=0$ corresponds to the transmitted laser pulse through the sample. As shown by the dotted lines in Fig. 1, overlap between the laser pulse spectrum and the exciton spectra is very small and most of the laser field is freely transmitted through the sample. The trailing tail of the signal is multiplied by 150, and clear oscillatory structure appears. The structure is attributed to the quantum beat of $n=2$, 3, and 4 excitons.

Figure 3 shows the FID signal from the $n=1$ exciton. Although the signal expected from a single peak is a simple exponential decay curve, the experimental result shows completely different features. Notable features are

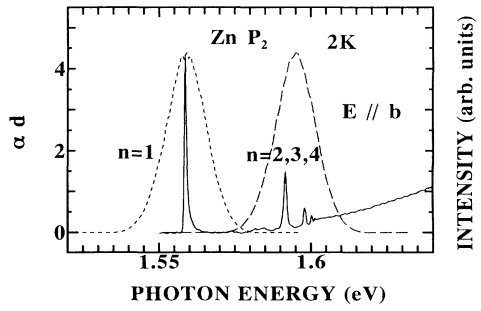

FIG. 1. Absorption spectrum of a ZnP_2 single crystal at 2 K for $E \parallel b$ polarization. Sharp Wannier excitons up to $n=4$ are clearly seen. The short and long dashed lines are spectra of the femtosecond laser pulses used in the experiment and cover the $n=1$ and $n=2,3,4$ exciton peaks, respectively.

0031-9007/93/71(17)/2785(4)$06.00

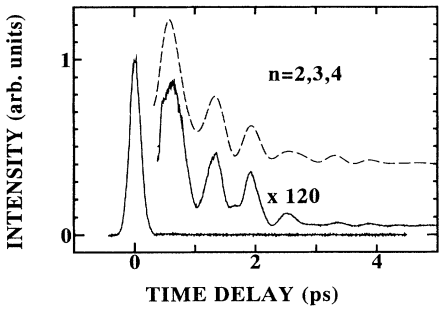

FIG. 2. Free induction decay signal from the $n=2,3,4$ excitons. The large peak at the time origin corresponds to the transmitted laser pulse. The trailing edge is explained by a factor of 120 and the oscillatory signal appears clearly. The dotted line is a theoretical fit based on the excitonic quantum beats. Parameter values are $f_2:f_3:f_4=1:0.28:0.07$, $\omega_2=2.4183$ fs^{-1}, $\omega_3=2.4278$ fs^{-1}, $\omega_4=2.4313$ fs^{-1}, $\gamma_2=0.6$ ps^{-1}, $\gamma_3=0.5$ ps^{-1}, and $\gamma_4=0.3$ ps^{-1}.

a deep dip near the time origin and the oscillatory structure in the trailing tail. These effects are explained by the nonzero effects of time and space. In order to understand the experimental result, we derive the theoretical expressions for the free induction decay signal.

The optical field inside the resonant medium forms a polariton which is a hybrid state of photon and exciton states. By using the dielectric constant ε of the medium, the dispersion relation of the polariton is expressed as

$$\varepsilon(\omega)[ck(\omega)/\omega]^2, \tag{1}$$

where c, k, and ω are the velocity of light in vacuum, momentum, and energy of the polariton, respectively. Once the complex wave vector k of the polariton is obtained as a function of ω, the propagation effect of the polariton inside the medium is expressed as

$$G(\omega)=E_{\text{out}}(\omega)/E_{\text{in}}(\omega)=\exp[ik(\omega)d], \tag{2}$$

where d is the thickness of the sample, and the $E_{\text{in}}(\omega)$ and $E_{\text{out}}(\omega)$ are the complex Fourier component of the polariton at the entrance and the exit surfaces of the sample, respectively. This relation is easily rewritten in the time domain

$$E_{\text{out}}(t)=\int_{-\infty}^{+\infty} d\tau G(\tau)E_{\text{in}}(t-\tau), \tag{3}$$

where $E_{\text{out}}(t)$, $E_{\text{in}}(t-\tau)$, and $G(\tau)$ are the Fourier transform of $E_{\text{out}}(\omega)$, $E_{\text{in}}(\omega)$, and $G(\omega)$, respectively. If the incident optical field is short enough to be approximated by a δ function, $E_{\text{out}}(t)$ can be taken as $G(t)$. The intensity of transmitted light is given as

$$I(t)\propto|E_{\text{out}}(t)|^2. \tag{4}$$

To fit the experimental result, we use the simple harmonic oscillator model for the exciton system. The dielectric parameter of the material around sharp resonance lines is

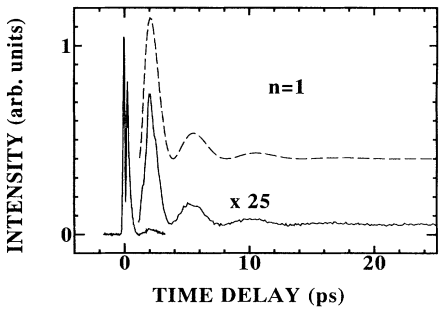

FIG. 3. The free induction decay signal from the $n=1$ exciton. The trailing edge is expanded by a factor of 25. Characteristic features are the oscillatory structure in the delayed region and a deep dip near the time origin. The dotted line represents a theoretical fit based on polariton beats. Parameter values $g=10$, $\omega_1=2.3679$ fs^{-1}, and $\gamma_1=0.05$ ps^{-1} were used.

$$\varepsilon(\omega)=\varepsilon_b+\frac{e^2}{m}\sum_n\frac{f_n}{\omega_n^2-\omega^2-2i\gamma_n\omega}, \tag{5}$$

where ε_b, e, and m are the background dielectric constant, charge, and mass of the electron, respectively and f_n, ω_n, and γ_n are the oscillator strength, resonant frequency, and damping constant of the nth resonance line, respectively. Assuming that the second resonant term is much smaller than the first background term, $k(\omega)$ can then be approximated as

$$k(\omega)=\frac{\omega}{c}\sqrt{\varepsilon_b}+\frac{e^2}{4mc\sqrt{\varepsilon_b}}\sum_n\frac{f_n}{\omega_n-\omega-i\gamma_n}. \tag{6}$$

The first term corresponds to the simple propagation time delay and a significant pulse deformation comes from the second term. Omitting the first term in Eq. (6), we can get two limiting cases as follows. If $k(\omega)d$ is much smaller than 1, then Eq. (2) is approximated by $1+ik(\omega)d$. This is the case for exciton quantum beats of the $n=2$, 3, and 4 excitons. The corresponding $G_{\text{QB}}(\tau)$ for the exciton quantum beat is

$$G_{\text{QB}}(\tau)=\delta(\tau)-\frac{e^2d}{4mc\sqrt{\varepsilon_b}}\times\sum_{n=2}^{4}f_n\theta(\tau)\exp[-(\gamma_n+i\omega_n)\tau], \tag{7}$$

where $\theta(\tau)$ is a step function. For the $n=1$ exciton, $k(\omega)d$ is of the same order of 1 and we cannot simplify Eq. (2) anymore. In this case, we can obtain the expression for the polariton beat as

$$G_{\text{PB}}(\tau)=\frac{1}{2\pi}\int_{-\infty}^{+\infty}d\omega\exp(-i\omega\tau)\exp\left[i\frac{g}{\omega_1-\omega-i\gamma_1}\right], \tag{8}$$

where

$$g=\frac{e^2}{2mc\sqrt{\varepsilon_b}}f_1d.$$

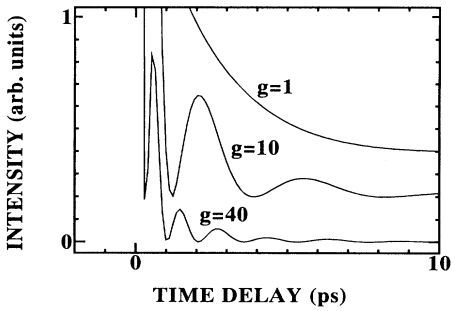

FIG. 4. Plots of $|G_{PB}(t)|^2$ for several g values. ω_l and γ_l are 2.3679 fs^{-1} and 0.05 ps^{-1}, respectively. For small values of g, the signal exponentially decreases. As g increases, oscillatory structure appears.

We thus obtain two forms of the FID signal, as given in Eqs. (7) and (8). The square of the absolute values of G_{QB} and G_{PB} directly gives the FID signals, and the best fits are presented in Fig. 2 and Fig. 3 by dotted lines. In this way, both the exciton beat and the polariton beat are explained by simple formulas.

In Fig. 4, the time profiles of $|G_{PB}(t)|^2$ for several g values are plotted. The value of γ_l is taken as 0.05 ps^{-1} for all the curves. For the g value of 1 ps^{-1}, the curve shows nearly exponential decay. As g increases, the curves show oscillatory structures which is explained by the interference between the upper and the lower polariton branches [13].

The deep dip around the time origin originates from the nonzero pulse width of the nearly Fourier-transform-limited pulse. To evaluate the coherent dip, a δ-function approximation of the input pulse shape cannot be adopted, and we must calculate Eq. (3) using appropriate input pulse shape. In Fig. 5(a), the FID signal for the $n=1$ exciton around the time origin is displayed. In Fig. 5(b), numerical calculations are shown. The short and long dashed lines correspond to the intensities of the input optical field and the optical field emitted by the exciton, respectively. We used a 130-fs sech^2 shape for the input pulses. The optical field emitted by the exciton is calculated as $E_{out}(t)-E_{in}(t)$. The rise of exciton emission intensity corresponds to the growth of polarization and coincides with the integration of the input pulse. The incident optical field and the emitted one have opposite optical phases except for the negligible phase shift caused by decay and propagation. This canceling interference causes the coherent dip and this is just how the excitons absorb the optical field. The solid line in Fig. 5(b) shows the intensity of the output optical field $E_{out}(t)$. The time broadening caused by the optical mixing technique is not included in the data. Even when the broadening is properly convoluted, a difference between the experimental curve in Fig. 5(a) and the theoretical curve in Fig. 5(b) still remains. The theoretical curve is strongly dependent on the shape of the input pulse. The observed difference is attributed to both the pulse shape of the laser and the

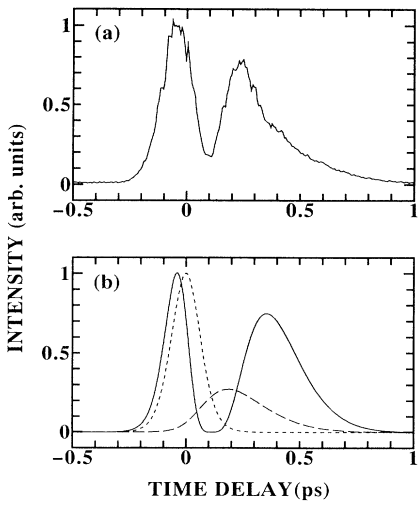

FIG. 5. Coherent dip effects. (a) Experimental result, (b) theoretical calculation. The short and long dashed lines shown in (b) are the intensities of the input optical pulse and the emitted field from the excitons, respectively. The rise of the exciton signal originates from the time integration of an input pulse. The two components have almost opposite phases and the combined output signal shows a deep dip structure.

breakdown of the harmonic oscillator model.

In spite of a small overlap of the laser spectrum and exciton spectrum, as shown in Fig. 1, the FID signal is of the same order of magnitude as the incident field. This is not surprising, because a sharp resonance line can absorb and emit a nonresonant optical field transiently within the uncertainty relation of time and frequency. The time-resolved signal gives the transient absorption and emission of light fields which does not necessarily mean energy loss, whereas the static absorption spectrum gives the energy loss inside the sample.

In this way, our experimental result is well explained by simple equations. It is noted that the simplicity results from the small oscillator strength of excitons in ZnP_2. Weak oscillator strength and a thick sample allow realization of an almost boundary-free condition. Actually, ε_b is 10 and no detectable reflection structure is observed around the exciton peaks in the reflection spectra. The flat reflection spectrum guarantees that there is no change of pulse shape at the boundaries. As a result, we can assume that the internal field is proportional to the external field at the boundaries and we can restrict our attention to the propagation effect. However, in general, the boundary conditions are very important, especially in samples with large oscillator strengths and in superlattices. To evaluate the FID signal in a general medium, we must consider its complicated boundary conditions [18,19].

In conclusion, we have investigated the coherent propagation of femtosecond pulses in a ZnP_2 crystal. The experimental result shows that the simple resonance line leads to an unexpected time evolution of the polariton

beat and the coherent dip. The result is well explained by simple equations. This demonstrative experiment shows that the coherent propagation effect is very important in femtosecond time-resolved experiments.

This work was supported by the Murate Science Foundation and Scientific Research Grant-in-Aid No. 03402007 and No. 04740156 from the Ministry of Education, Science, and Culture of Japan.

[1] L. Schultheis, M. D. Sturge, and J. Hegarty, Appl. Phys. Lett. **47**, 995 (1985).

[2] L. Schultheis, J. Kuhl, A. Honold, and C. W. Tu, Phys. Rev. Lett. **57**, 1635 (1986).

[3] C. Dörnfeld and J. M. Hvam, IEEE J. Quantum Electron. **25**, 904 (1989).

[4] K. Leo, M. Wegener, J. Shah, D. S. Chemla, E. O. Göbel, T. C. Damen, S. Schmitt-Rink, and W. Schäfer, Phys. Rev. Lett. **65**, 1340 (1990).

[5] K. Leo, T. C. Damen, J. Shah, E. O. Göbel, and K. Köhler, Appl. Phys. Lett. **57**, 19 (1990).

[6] E. O. Göbel, K. Leo, T. C. Damen, S. Schmitt-Rink, W. Schäfer, J. F. Müller, and K. Köhler, Phys. Rev. Lett. **64**, 1801 (1990).

[7] B. F. Feuerbacher, J. Kuhl, R. Eccleston, and K. Ploog, Solid State Commun. **74**, 1279 (1990).

[8] S. Bar-Ad and I. Bar-Joseph, Phys. Rev. Lett. **66**, 2491 (1991).

[9] E. L. Hahn, Phys. Rev. **77**, 297 (1950).

[10] R. G. Brewer and R. L. Shoemaker, Phys. Rev. A **6**, 2001 (1972).

[11] Hyatt M. Gibbs, Phys. Rev. Lett. **29**, 459 (1972); see also Hyatt M. Gibbs, Phys. Rev. A **8**, 446 (1973).

[12] L. Allen and J. H. Eberly, *Optical Resonance and Two-level Atoms* (Wiley, New York, 1975).

[13] D. Fröhlich, A. Kuik, B. Uebbing, A. Mysyrowicz, V. Langer, H. Stolz, and W. von der Osten, Phys. Rev. Lett. **67**, 2343 (1991).

[14] K.-H. Pantke, P. Schillak, B. S. Razbirin, V. G. Lyssenko, and J. M. Hvam, Phys. Rev. Lett. **70**, 327 (1993).

[15] A. B. Pevtsov, S. A. Permogorov, A. V. Sel'kin, N. N. Syrbu, and A. G. Umanets, Fiz. Tekh. Poluprovodn. **16**, 1399 (1982) [Sov. Phys. Semicond. **16**, 897 (1982)].

[16] S. Taguchi, T. Goto, M. Takeda, and G. Kido, J. Phys. Soc. Jpn. **57**, 3256 (1988); see also T. Goto, S. Taguchi, Y. Nagamune, S. Takeyama, and N. Miura, J. Phys. Soc. Jpn. **58**, 3822 (1989); see also T. Goto, S. Taguchi, K. Cho, Y. Nagamune, S. Takeyama, and N. Miura, J. Phys. Soc. Jpn. **59**, 773 (1990).

[17] O. Arimoto, S. Okamoto, and K. Nakamura, J. Phys. Soc. Jpn. **59**, 3490 (1990); see also O. Arimoto, H. Takeuchi, and K. Nakamura, Phys. Rev. B **46**, 15512 (1992).

[18] S. I. Pekar, Zh. Eksp. Teor. Fiz. **33**, 1022 (1957) [Sov. Phys. JETP **6**, 785 (1958)].

[19] K. Cho, J. Phys. Soc. Jpn. **55**, 4113 (1986).